Plug-and-Play Model Predictive Control for Load Shaping and Voltage Control in Smart Grids

Caroline Le Floch[a], Somil Bansal[b], Claire J. Tomlin[b], Scott Moura[a], Melanie N. Zeilinger[c]

***Abstract*—This paper presents a predictive controller for handling plug-and-play (P&P) charging requests of flexible loads in a distribution system. Two types of flexible loads are defined: (i) deferrable loads that have a fixed power profile but can be deferred in time and (ii) shapeable loads that have flexible power profiles but fixed energy requests, such as Plug-in Electric Vehicles (PEVs). The proposed method uses a hierarchical control scheme based on a model predictive control (MPC) formulation for minimizing the global system cost. The first stage computes a reachable reference that trades off deviation from the nominal voltage with the required generation control. The second stage uses a price-based objective to aggregate flexible loads and provide load shaping services, while satisfying system constraints and users' preferences at all times. It is shown that the proposed controller is recursively feasible under specific conditions, i.e. the flexible load demands are satisfied and bus voltages remain within the desired limits. Finally, the proposed scheme is illustrated on a 55 bus radial distribution network.**

***Index Terms*—Electric Vehicles, Load shedding, Mixed integer programming, Plug and play model predictive control, Scheduling, Voltage control.**

I. INTRODUCTION

The development of smart meters has led to the modernization of distribution networks by enabling real-time bidirectional communication [1]. In this context of smart grids, demand side management allows system operators to control the energy consumption at the household level, offering new opportunities to improve the reliability, efficiency and sustainability of the grid [2], [3]. In particular, automated load shifting is expected to play a key role in stabilizing the grid in the case of high penetration of plug-in Electric vehicles (PEVs) and uncontrollable renewable sources, such as photovoltaic solar energy [4], [5].

PEVs provide a compelling opportunity for supplying demand-side management services in the smart grid. For example, a vehicle-to-grid (V2G) capable PEV can communicate with the grid, can store energy, and can transfer energy back to the electric grid when required [6], [7], [8]. Other flexible commercial and residential loads such as thermostats, controllable lighting or dishwashers can be deferred to adapt their consumption according to the distribution grid constraints. The main challenge, however, is managing a large population of distributed loads while ensuring (i) computational tractability, (ii) user satisfaction, and (iii) power system constraints.

A growing body of literature addresses optimal load scheduling to provide demand response services. In particular, many efficient distributed algorithms have been proposed to address only the scheduling problem, but neglecting distribution grid constraints [9], [10], [11]. However, these approaches may result in overloading of the lines and infeasible solutions for the distribution grid [12]. The authors in [12], [13] propose decentralized strategies to provide ancillary services while considering capacity constraints and transformer overheating, but do not consider voltage constraints. Yet, with the growing penetration of renewable and distributed resources, the risk of voltage instability and reverse power flow increases, and it becomes essential to coordinate loads by considering the extensive set of distribution grid constraints. The goal of this paper is to develop a control scheme that integrates flexible loads in the existing distribution network, provides local and aggregated grid services and satisfies users' requirements, as well as grid constraints.

There are two key challenges in designing such a controller. First, it should be able to handle variations in the number of connected loads, i.e. plugging in and out operations. In a real scenario, a user can request to connect or disconnect any load at any desired time and bus. Modeling all the possible requests results in a very large scale and uncertain system, which has been studied through model predictive control (MPC) [14], maximum sensitivity selection [15], and solved by using parallel computing methods [16]. These solutions with fixed-order models (centralized or distributed) do not account for changes in state dimension when PEVs plug-in and plug-out. In contrast, the proposed framework models only the static state of the network and deals with plug-in requests when new loads require supply. Contrary to most available results, the proposed controller is not based on flexible load forecasting, but is redesigned each time a new load is connected. Second, the controller should consider two different objectives and time scales: local voltage regulation and aggregate load shaping. Previous work has proposed multilevel and multi-horizon approaches [14], [17], [18] and decentralized protocols [13] but does not consider the available distribution grid control devices. In opposition, this paper does not only include the state of the network, but also the control of battery banks and capacitors, which are jointly optimized with the load profiles.

The proposed solution is based on a two-stage plug-and-play model predictive controller. While the main focus of MPC so far has been on the control of networks with constant

This work was funded in part by the Siebel Energy Institute, the Swiss National Science Foundation and the National Science Foundation within the Division of Electrical, Communications and Cyber Systems under Grant 1408107.

[a]Civil and Environmental Engineering, University of California, Berkeley, United States, caroline.le-floch@berkeley.edu

[b]Electrical Engineering and Computer Sciences, University of California, Berkeley, United States

[c]Mechanical and Process Engineering, ETH Zurich, Switzerland

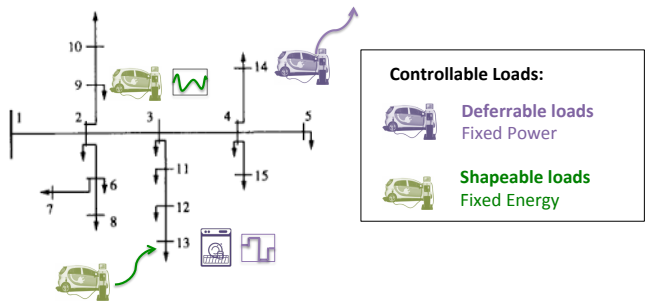

Fig. 1. Schematic representation of the protocol: loads plugging in and out of the distribution network.

topology, the concept of plug and play (P&P) MPC [19], [20], [21] considers network changes by subsystems that want to join or leave the network, while ensuring feasibility and stability of the global system. By providing an automatic redesign of the control laws in response to changing network conditions, P&P MPC is an attractive scheme for modern control systems of increasing complexity. We provide a P&P framework to deal with the connection and disconnection of loads from the grid, which requires an online feasibility handling as introduced in [22]. Compared to previous work in [22], which considers voltage control in a distribution grid, we propose a methodology to control loads with fixed charging deadlines, and achieve both load shaping and voltage control. A procedure for updating the controller together with a transition scheme is proposed, which prepares the system for the requested modifications, and we provide a new proof of recursive feasibility, i.e. satisfaction of network constraints and user deadlines. A schematic representation of the protocol is given in Fig. 1.

To summarize, the main contributions of this paper are:

- It presents a P&P MPC scheme that optimally schedule loads to be connected and shape current loads while satisfying network constraints at all times. The Second Order Cone relaxation of the DistFlow equations (see [23]) is used to model power flows in the distribution network, and improve the accuracy of the model compared to the linear approximation used in [22].
- The controller is applicable to different types of loads. In particular, two types of loads are defined: deferrable loads that can be delayed but have a fixed profile, and shapeable loads that have a flexible profile but need a fixed amount of energy. The proposed algorithm satisfies users' requirements by ensuring that every flexible load reaches the desired energy level at the desired time and any deferrable load demand is met before its deadline.

The paper is organized as follows: Section II introduces the system model. In Section III, control objectives are defined and the hierarchical MPC controller is proposed. Section IV provides an extension for handling plug and play requests. Section V presents numerical simulations demonstrating the advantages of the proposed control scheme and Section VI provides concluding remarks.

II. PRELIMINARIES

This section introduces the different elements of the network, including deferrable and shapeable loads, battery banks and capacitors. The overall system is modeled as a constrained dynamic system with linear dynamics and energy constraints.

A. Load modeling

Let consider a load with proposed energy profile $e(k)$ and power profile $c(k)$, where k is the discrete time step. The role of the scheduling operator is to generate another energy profile $\widetilde{e} = \tau(e)$. Three types of loads with different maps τ are distinguished (see Fig. 1):

- *Fixed loads* do not participate in demand response and cannot be controlled : $\widetilde{e}^f(k) = e^f(k)$.
- *Deferrable loads* can be delayed but have a fixed load profile. In this case $\widetilde{e}^{def}(k) = e^{def}(k-d)$ with d bounded by a constraint on the maximum allowable delay. This includes PEVs with constant charging rate.
- *Shapeable loads* have a flexible profile but need a fixed amount of energy in a fixed time period T: $\sum_{k=0}^{T} \widetilde{e}^{shp}(k) = \sum_{k=0}^{T} e^{shp}(k)$. It includes PEVs with continuous charging rate.

In the following sections, we model the load dynamics. For simplicity, only real power loads are considered in the remainder of this paper. Reactive loads could be introduced in a similar fashion, where capacitors would play the role of battery banks.

TABLE I
NOMENCLATURE - LOAD DYNAMICS

Symbol	Description
Variables	
$e^{def}(k)$	Deferrable load energy level at time k (kWh)
$c^{def}(k)$	Deferrable load power at time k (kW)
$e^{shp}(k)$	Shapeable load energy level at time k (kWh)
$e^{shp}_{min}(k)$	Minimum shapeable load energy at time k (kWh)
$c^{shp}(k)$	Shapeable load power at time k (kW)
$e^{bat}(k)$	Battery energy level at time k (kWh)
$p^{bat}(k)$	Battery power at time k (kW)
Parameters	
ΔT	Duration of time step $(1/h)$
η^{def}	Deferrable load efficiency coefficient (1)
c_0^{def}	Deferrable load fixed power profile (kW)
η	Shapeable load efficiency coefficient (1)
e^{shp}_{low}	Shapeable load energy physical lower limit (kWh)
e^{shp}_{max}	Shapeable load energy physical maximum limit (kWh)
e^{shp}_{des}	Shapeable load desired energy level (kWh)
c^{shp}_{max}	Shapeable load maximum power (kW)
k^{out}	Charging deadline (h)
p^{bat}_{max}	Battery maximum power (kW)
p^{bat}_{min}	Battery minimum power (kW)

1) Deferrable loads: Consider a deferrable load with a proposed power profile $c_0^{def}(k) > 0$ (see Ref [24], [25] for typical profile examples). As soon as the deferrable load plugs in, its power profile c^{def} becomes deterministic:

$$e^{def}(k+1) = e^{def}(k) + \eta^{def} \Delta T c^{def}(k) \quad (2a)$$

$$c^{def}(k) = c_0^{def}(k) \quad (2b)$$

In Eq (2a), ΔT and $\eta^{def} \leq 1$ are parameters corresponding respectively to the duration of time intervals and the efficiency coefficient, which accounts for energy conversion losses.

Remark 1. *The only control on deferrable loads comes from P&P operations, which determines when to plug-in the load. After it is connected, the load is deterministic and can be considered as a fixed load.*

2) Shapeable loads:
Power at shapeable loads c^{shp} can take values in a continuous range $[0, c^{shp}_{max}]$. We define e^{shp}_{low}, e^{shp}_{max} and e^{shp}_{des} as the physical lower limit, physical upper limit and desired energy level of the load, respectively. The dynamics of shapeable loads are given by:

$$e^{shp}(k+1) = e^{shp}(k) + \eta \Delta T c^{shp}(k) \quad (3a)$$
$$e^{shp}_{min}(k) \leq e^{shp}(k) \leq e^{shp}_{max} \quad (3b)$$
$$0 \leq c^{shp}(k) \leq c^{shp}_{max} \quad (3c)$$

where $\eta < 1$ is an efficiency parameter. The user's constraint implies that the load is fully charged by time k^{out}, where k^{out} is a parameter communicated to the controller when the load requests supply: $e^{shp}(k^{out}) \geq e^{shp}_{des}$. As a result, the lower bound constraint $e^{shp}_{min}(k)$ is due to two independent factors: (i) the user's constraint in Eq (4), and (ii) the physical energy lower limit in Eq (5):

$$e^{shp}_{min}(k) \geq e^{shp}_{des} - (k^{out} - k) c^{shp}_{max} \Delta T \eta \qquad \forall k \leq k^{out} \quad (4)$$
$$e^{shp}_{min}(k) \geq e^{shp}_{low} \quad \forall k \quad (5)$$

Equations (4) and (5) can be combined as follows:

$$e^{shp}_{min}(k) = \max[e^{shp}_{des} - \max(0, (k^{out} - k) c^{shp}_{max} \eta \Delta T), e^{shp}_{low}]. \quad (6)$$

In the remainder of this paper we use the notation:

$$1_{k<k^{out}} = \begin{cases} 1 & \text{if } k < k^{out} \\ 0 & \text{otherwise} \end{cases}$$

B. Battery banks

On-site batteries are modeled with a linear state space model:

$$e^{bat}(k+1) = e^{bat}(k) + \Delta T p^{bat} \quad (7a)$$
$$e^{bat}_{low} \leq e^{bat}(k) \leq e^{bat}_{max} \quad (7b)$$
$$p^{bat}_{min} \leq p^{bat}(k) \leq p^{bat}_{max} \quad (7c)$$

where e^{bat}_{low}, e^{bat}_{max} are the fixed physical lower and upper limits of the battery's energy level and p^{bat}_{min}, p^{bat}_{max} are the minimum and maximum power. This model assumes perfect battery efficiency, which is a simplified approximation of the battery dynamics. The introduction of an efficiency factor $\eta < 1$ would result in a non-convex program as shown in [26], [27]. As a result, the perfect efficiency assumption in (Eq 7) is frequently used in the power system literature to formulate the overall system as a linear dynamical system, and to simplify the resulting control scheme ([28], [22], [29]).

C. Network Model

We consider a radial distribution network, which is a structure commonly used in the power systems literature. To characterize the power flow in this network we adopt the DistFlow equations first introduced in [30] and the notation introduced in [31], restated here for completeness.

TABLE II
NOMENCLATURE - RADIAL DISTRIBUTION NETWORK

Symbol	Description
Sets	
$\mathcal{N}$	Set of buses, $\mathcal{N} := \{1, \ldots, n\}$
$\mathcal{L}$	Set of lines between the buses in $\mathcal{N}$
$\mathcal{L}_i$	Set of lines connecting bus 0 to bus i
Parameters	
M_i	Number of shapeable loads connected at bus i
Variables	
p^l_i	Real power consumption by fixed loads at bus i (kW)
p^{bat}_i	Real power consumption by battery banks at bus i (kW)
p^{shp}_i	Real power consumption by shapeable loads at bus i (kW)
p^{def}_i	Real power deferrable loads at bus i (kW)
q^l_i, q^g_i	Reactive power consumption and generation at bus i (Var)
r_{ij}, x_{ij}	Resistance and reactance of line $(i,j) \in \mathcal{L}\Omega$
P_{ij}, Q_{ij}	Real and reactive power flows from bus i to j (kW, Var)
v_i	Voltage magnitude at bus i (V)
L_{ij}	Squared magnitude of complex current from bus i to j (A^2)

The power flow equations for a radial distribution network can be written as the following DistFlow equations [32]:

$$P_{ij} = p^l_j + p^{bat}_j + p^{def}_j + p^{shp}_j + r_{ij} L_{ij} + \sum_{k:(j,k)\in\mathcal{L}} P_{jk} \quad (8a)$$
$$Q_{ij} = q^l_j - q^g_j + x_{ij} L_{ij} + \sum_{k:(j,k)\in\mathcal{L}} Q_{jk} \quad (8b)$$
$$v^2_j = v^2_i + (r^2_{ij} + x^2_{ij}) L_{ij} - 2(r_{ij} P_{ij} + x_{ij} Q_{ij}) \quad (8c)$$
$$L_{ij} v^2_i = P^2_{ij} + Q^2_{ij} \quad (8d)$$
$$\forall j \in \mathcal{N} \backslash \{1\}, \text{ and } (i,j) \in \mathcal{L}$$

where P_{ij}, Q_{ij}, v_j and L_{ij} are defined in Table II. Because the above formulation is non-convex, the Second Order Cone relaxation (SOCP) defined in [23] is used, and equation (8d) is relaxed as follows:

$$L_{ij} \geq \frac{P^2_{ij} + Q^2_{ij}}{v^2_i}. \quad (9)$$

The variables are the reactive power generation input (column) vector $q^g := (q^g_1, \ldots, q^g_n) \in \mathbb{R}^n$, the battery input vector $p^{bat} := (p^{bat}_1, \ldots, p^{bat}_n) \in \mathbb{R}^n$ and the shapeable, deferrable and fixed loads: p^{shp}, p^{def}, $p^l \in \mathbb{R}^n$, where $p^{shp}_i \in \mathbb{R}^+$ and $p^{def}_i \in \mathbb{R}^+$ denote the net shapeable loads and net deferrable loads charging at bus i, respectively. Symbols M^{shp}_i and M^{def}_i denote the number of shapeable and deferrable loads connected at bus i, respectively. These values can vary over time due to plugging and unplugging operations. This relates with the notation in Section II-A as follows:

$$p^{shp}_i = \sum_{j=1}^{M^{shp}_i} c^{shp}_j, \qquad p^{def}_i = \sum_{j=1}^{M^{def}_i} c^{def}_j \quad (10)$$

The substation voltage v_0 is assumed to be given and constant. Furthermore, load profiles p^l and q^l are time-varying but their 24-hour forecast is assumed to be given.

D. Network Constraints

Depending on the load, bus voltages can fluctuate significantly. For reliable operation of the distribution network, it is required to maintain the bus voltages v within a tight range around the nominal value v_{nom} at all times (generally 5% deviation): $v_{nom} - \Delta v_{max} \leq v \leq v_{nom} + \Delta v_{max}$. We define the variable $V_i = v_i^2$ and write this condition as:

$$V_{min} \leq V_i \leq V_{max}. \tag{11}$$

Moreover, storage devices can supply energy at the nodes of the network when $P_{bat} < 0$, which may introduce reverse power flow in the lines [33] and create operational issues in traditional power networks [34]. This issue is avoided by imposing the following constraint:

$$P_{ij} \geq 0 \quad \forall (i,j) \in \mathscr{L} \tag{12}$$

In addition, there are inherent physical limitations on the capacitor control input, which is limited to:

$$q_{min} \leq q^g \leq q_{max}. \tag{13}$$

E. Dynamic System

In this section, the overall system is represented as a constrained dynamic system with energy levels as states. Recalling that $p_i^{shp} = \sum_{j=1}^{M_i^{shp}} c_j^{shp}$, we can write $p^{shp} = K^{shp} u^{shp}$ where $u^{shp} := (c_1^{shp}, \ldots, c_{M^{shp}}^{shp})^T \in \mathbb{R}^{M^{shp}}$, and M^{shp} is the total number of shapeable loads connected to the grid, i.e. $M^{shp} = \sum_{j=1}^{n} M_j^{shp}$. Matrix $K^{shp} \in \mathbb{R}^{n \times M^{shp}}$ is defined such that:

$$K_{ij}^{shp} = \begin{cases} 1 & \text{if shapeable load j is connected to bus i} \\ 0 & \text{otherwise} \end{cases}$$

The overall system model is described as follows:

$$x(k+1) = Ax(k) + Bu(k) \tag{14a}$$
$$(x(k), u(k)) \in \mathscr{Z}_k \tag{14b}$$

$$x = \begin{bmatrix} x_1, x_2 \end{bmatrix}^T = \left[(e_1^{shp}, \ldots, e_{M^{shp}}^{shp}), (e_1^{bat} \ldots, e_n^{bat}) \right]^T$$
$$u = \begin{bmatrix} q^g & u^{shp} & p^{bat} \end{bmatrix}^T$$

$$A = I, \quad B = \begin{bmatrix} 0 & \eta \Delta T & 0 \\ 0 & 0 & \Delta T \end{bmatrix}$$

$$\begin{aligned} \mathscr{Z}_k = \{ & (x(k), u(k), P_{ij}(k), Q_{ij}(k), V_i(k), L_{ij}(k)) : \\ & (8a), (8b), (8c), (9), (12), \\ & V_{mini}(k)_{max}, \quad e_{min}(k) \leq x(k) \leq e_{max}, \\ & p_{min}^{bat} \leq p^{bat} \leq p_{max}^{bat}, \quad q_{min} \leq q^g(k) \leq q_{max}, \\ & 0 \leq u^{shp}(k) \leq c_{max}^{shp} \}. \end{aligned}$$

III. Controller Design

The controller is designed with three control objectives:

- *Peak reduction*: Smooth the aggregated power profile.
- *User satisfaction*: Provide the desired energy to shapeable and deferrable loads.
- *Voltage control*: Ensure that voltage deviation from nominal voltage remains within bounds.

For the purpose of this section, the number of loads connected to the grid is assumed constant. Plug and play connections are introduced in Section IV.

A. Stage 1: Feasible reference

In the remainder of this paper, Eq. (14) with $p^{def} = 0$, $u^{shp} = 0$ refers to the dynamics with no deferrable and no shapeable loads. We assume that the system has a feasible trajectory and has the following periodic property, with period N_r:

Assumption 1. *There exists an initial value $\hat{x}_0$ and a sequence of control inputs $\hat{u}(k)$, such that the corresponding sequence of states $\hat{x}(k)$ according to dynamics (14a) with $p^{def} = 0$, $u^{shp} = 0$ satisfies the constraints in (14b), i.e. $(\hat{x}(k), \hat{u}(k)) \in \mathscr{Z}_k$ for all $k \in \{0, ..., N_r - 1\}$.*

Assumption 2. *If problem (14) with $p^{def} = 0$, $u^{shp} = 0$, $x(k) = x_0$ is feasible at time k, then problem (14) with $p^{def} = 0$, $u^{shp} = 0$, $x(k+N_r) = x_0$ is feasible at time $k+N_r$.*

In practice, Assumption 1 means that the traditional control devices (battery banks and capacitors) are selected according to the traditional fixed loads p^l. When new loads, such as PEVs, are not plugged-in, traditional control devices have enough flexibility to regulate voltage. Assumption 2 means that if the problem is feasible at time k, then the problem with same initial state is feasible at time $k+N_r$, where the period N_r is typically a day. Deferrable and shapeable loads increase power demand and voltage drop, which requires extra control capacity. In this case, the problem with extra loads may not be feasible, requiring to solve the problem in a hierarchical way. First an optimal solution is computed for the system without extra loads, second this reference signal is used to formulate a model predictive controller. The optimization problem for computing the solution with only fixed loads $(\hat{x}(k); \hat{u}(k))$ is referred to as *stage-1* in this paper:

$$(\hat{x}(k), \hat{u}(k)) := \underset{\tilde{x}, \tilde{u}}{\operatorname{argmin}} \sum_{i=0}^{N_r - 1} ||\tilde{u}(i)||_{T_1}^2 + ||V(i) - V_{nom}||_{T_2}^2$$
$$\text{s.t.} \quad \tilde{x}(i+1) = A\tilde{x}(i) + B\tilde{u}(i) \tag{15a}$$
$$\tilde{x}(0) = A\tilde{x}(N_r - 1) + B\tilde{u}(N_r - 1) \tag{15b}$$
$$(\tilde{x}(i), \tilde{u}(i)) \in \mathscr{Z}_i; \quad i = 0, \ldots, N_r - 1 \tag{15c}$$
$$M^{def} = M^{shp} = 0$$

where T_1 and T_2 are respectively positive definite and positive semi-definite weight matrices of appropriate dimensions (see [35, Chapter 1] for details about weighted norms). The terminal constraint (15b) ensures that batteries recover their initial energy level at the end of the control horizon.

Remark 2. *At* stage-1*, a cost function is chosen that penalizes the generation control input and the deviation of voltage from its nominal value. The matrix T_2 is defined positive semi-definite since tracking the nominal voltage improves the power quality for loads, but the constraint (15c) is enough to ensure that voltage remains between operational bounds at every time step $i \in \{0,\dots,N_r-1\}$.*

B. Stage 2: Model Predictive Controller

In the second stage, a predictive controller is designed to minimize the overall cost of the system for time steps in $\{0,..,N-1\}$, with $N < N_r$. Problem *stage-1* is computed once, at the begining of the horizon, and the corresponding solution is used to ensure that the *stage-2* problem remains recursively feasible under a receding horizon strategy. Let $\lambda(t)$ denote the price of electricity at time t. The price $\lambda(t)$ is given as an input to the MPC and reflects demand peaks and congestion in the grid. This price can change at every time step, and reflect dynamic price markets. We propose the following MPC problem (referred to as *stage-2* in this paper):

$$\min_{x,u} \quad \sum_{i=0}^{N-1} \lambda(i+k)\Big(\sum_{j=1}^{M^{shp}} u_j^{shp}(i+k)\Big) + ||V - V_{nom}||^2_{T_3} \quad (16a)$$

$$\text{s.t} \quad x(i+1+k) = Ax(i+k) + Bu(i+k) \quad (16b)$$

$$x(k) = x_k \quad (16c)$$

$$(x(i+k), u(i+k)) \in \mathscr{Z}_{i+k}; \quad i = 0,\dots,N-1 \quad (16d)$$

$$x(N+k) \in \mathbb{X}_{N+k} \quad (16e)$$

In the MPC problem (16), the first term achieves peak reduction through the time-varying price λ, while the second term penalizes voltage deviation. In the first term, the contribution from fixed loads p^l, and deferrable loads p^{def} is uncontrollable, therefore load shaping can only be achieved by controlling u^{shp}. The loads directly respond to the price, and it is beyond the scope of this paper to set the price λ. We refer to [4], [27] for methods to set this price. In the second term, the weight matrix T_3 is positive semi-definite and can be used to penalize large voltage deviations from v_{nom}.

Remark 3. *The solution from* stage-1 *is used to define the terminal set $\mathbb{X}_{N+k}$ in the next Section. Thus, the horizon time N is chosen such that $N < N_r$.*

C. Terminal Set

In this section, we detail the terminal set (16e). This constraint ensures that the system has enough flexibility to charge shapeable and deferrable loads before their plug-out time k^{out}, and keep voltage between the regular bounds after the control horizon N. The terminal set is defined such that the battery banks have enough energy to meet the real power demand of additional (shapeable and deferrable) loads at the end of horizon. Moreover, the capacitors supply the reactive power to satisfy the network constraints under base load. Feasibility of the *stage-1* problem thus ensures that all network constraints are satisfied even with the additional loads.

The terminal constraint for the shapeable loads' energy $x_1 = (e_1^{shp},\dots,e_{M^{shp}}^{shp})^T$ should guarantee that each load can be fully charged before their plug-out time. This is given by Eq. (6), which ensures the recursive feasibility of the constraint $e_{min}(k) \le x(k) \le e_{max}$, where $e_{min}(k^{out}) = e_{des}^{shp}$.

The terminal constraint for the battery banks' energy $x_2 = (e_1^{bat}\dots,e_n^{bat})^T$ guarantees that batteries have enough capacity at time N to track the reference signal from *stage-1* and supply the additional deferrable and shapeable loads. We denote $(\hat{q}_i,\ \hat{e}_i^{bat})$ the optimal solution to the *stage-1* problem in (15), and k_{max}^{out} the maximum plug-out time of all the deferrable and shapeable loads that are currently connected to the grid.

Definition 1. *The terminal set $\mathbb{X}_{N+k}$ at time $N+k$ is defined as follows:* $\mathbb{X}_{N+k} :=$

$$\begin{cases} \big[x_1(N{+}k), x_2(N{+}k)\big]^T = \big[e^{shp}(N+k), e^{bat}(N+k)\big]^T \\ \quad \textit{such that} \quad \forall i \in \{1,...,n\} \quad \forall j \in \{1,...,M^{shp}\} \\ \\ e_j^{shp}(N+k) \ge e_{des,j}^{shp} \text{ - } max(0,(k_j^{out} \text{ - } (N+k))\eta c_{max,j}^{shp}) \\ e_j^{shp}(N+k) \ge e_{low,j}^{shp} \\ \\ e_j^{shp}(N+k) \le e_{des,j}^{shp} \\ e_j^{bat}(N{+}\ k) = \hat{e}_i^{bat}(N{+}\ k) + \sum_{l=N+k}^{k_{max}^{out}} \Delta T\, p_i^{def}(l) + \tilde{p}_i^{shp}(l) \end{cases}$$

$$\tilde{p}^{shp}(l) \;=\; K^{shp}\tilde{c}^{shp}(l) \quad (17)$$

$$\tilde{c}_j^{shp}(l) \;=\; \frac{e_{des,j}^{shp} - e_j^{shp}(N+k)}{(k_j^{out} - (N+k))\eta\Delta T} 1_{l<k_j^{out}} \quad (18)$$

Lemma 1. *If the following conditions hold: $\forall l \in [N+k, k_{max}^{out}]$, $\forall i \in 1,...,n$:*

$$\hat{p}_i^{bat}(l) - p_i^{def}(l) - \tilde{p}_i^{shp}(l) \ge p_{imin}^{bat} \quad (19)$$

$$\hat{e}_i^{bat}(l) + \sum_{m=l}^{k_{max}^{out}} \Delta T\, p_i^{def}(m) + (e_{des,i}^{shp} - e_i^{shp}(N+k)) \frac{(k_i^{out} - l)}{\eta(k_i^{out} - (N+k))} \le e_{max,i}^{bat} \quad (20)$$

then problem (16) with terminal set $\mathbb{X}_{N+k}$ as defined in Definition 1, is recursively feasible, i.e. if the MPC optimization problem is feasible for $x(k)$, then it is also feasible for $x(k+1)$ defined in Eq. (14).

Proof. We provide an outline of the proof, which can be found in the extended version of this article in [36]. A feasible control sequence for *stage-2* at time $k+N$, $(p^{shp}(k+N), p^{bat}(k+N), q(k+N))$ is defined based on the solution of *stage-1* at time $k+N$, $(\hat{p}^{shp}(k+N), \hat{p}^{bat}k+(N), \hat{q}(k+N))$:

$$c_j^{shp}(N+k) \;=\; \frac{e_{des,j}^{shp} - e_j^{shp}(N+k)}{(k_j^{out} - (N+k))\eta\Delta T} 1_{N+k<k_j^{out}} \quad (21)$$

$$q_i(N+k) \;=\; \hat{q}_i(N+k) \quad (22)$$

$$p_i^{bat}(N+k) \;=\; [\hat{p}_i^{bat} \text{- } p_i^{def} \text{- } p_i^{shp}](N+k) \quad (23)$$

In practice, Eq (17) and (18) define a feasible control sequence after time $k+N$ where the shapeable power $\tilde{c}_j^{shp}$ at load j is constant until the plug-out time k_j^{out}. Then, Problem (16) is recursively feasible assuming that Equations (19), (20) are true (see [36]). □

Remark 4. *Lemma 1 shows that under conditions (19), (20) the MPC problem is feasible at all times, if it is feasible for an initial state x_0. The next section shows that the P&P operation ensures that conditions (19), (20) are always satisfied, proving constraint satisfaction at all times.*

IV. Plug-And-Play EV Charging

In real distribution systems, users can connect or disconnect their appliances randomly. This changes the overall load on the system and can affect bus voltages significantly. This section extends the MPC scheme to the case where the system dynamics in (14) change due to loads joining or leaving the network by employing the concept of P&P MPC in [20]. The introduction of P&P capabilities poses two key challenges ([20], [37]): (i) P&P operations may produce infeasible operating conditions; (ii) the control law has to be redesigned for the modified dynamics. In the considered case, the problem is reduced to the first issue since the controller is computed centrally by the *stage-2* MPC (Section III). In this section, the first challenge is addressed by means of a preparation phase ensuring recursive feasibility and stability during P&P operation. We first address the case of shapeable, then deferrable loads.

A. Shapeable loads

As shown in Eq. (3c), shapeable loads can be plugged-in without drawing energy from the grid: $0 \leq c^{shp} \leq c^{shp}_{max}$. Therefore it is always optimal for a shapeable load to plug-in as soon as it requests it: it can plug-in with $c^{shp} = 0$ and wait for the system to allow strictly positive values $c^{shp} > 0$. Thus, the output of the P&P stage is to accept shapeable requests immediately. Additionally, we assume that it is feasible to meet the user's requirements, i.e. fully charge the load before the maximum required time k^{out}, and satisfy equations (19), (20). In practice, if a user makes an infeasible request, he would be asked to lower his/her requirements by allowing a later k^{out} or a lower desired energy e^{shp}_{des}.

B. Deferrable loads

The goal of the P&P operation is to find a time to safely connect deferrable loads, and modify the response of shapeable loads and control devices to allow this connection as soon as possible. In this section, a Mixed Integer Program (MIP) is defined to find the minimum time to safely plug-in a deferrable load. After finding this time, the list of connected deferrable loads is updated, and *stage-2* is executed with the new system.

Deferrable loads do not impact the dynamics of the system, and only change the feasible set. An additional deferrable load at node j modifies the set $\mathscr{Z}_k$ via the equality:

$$P_{ij} = p^l_j + p^{bat}_j + p^{def}_j + p^{shp}_j + r_{ij}L_{ij} + \sum_{k:(j,k)\in\mathscr{L}} P_{jk}$$

Moreover, it modifies the terminal set $\mathbb{X}_{N+k}$. In the following, $\overline{\mathscr{Z}}_k$ (respectively $\overline{\mathbb{X}}_{N+k}$) denote the feasible set (respectively terminal set) constraints that remain unchanged when a deferrable load plugs in. Let's consider a P&P request from a deferrable load at time k. The request can be postponed by $d_{max} < N$ maximum time steps. This creates d_{max} possible load shapes. For each possible time-delay $0 \leq d \leq d_{max}$ we note $p^{new,d}_j$ the corresponding shifted vector:

$$p^{new,d}_j = [\underbrace{0,...,0}_{\text{size d}}, p^{new,0}_j] \tag{24}$$

Thus the following constraints are defined when a deferrable load requests to plug-in at node j and is delayed by d time steps:

$$\begin{aligned} P_{ij}(l) &= [p^l_j + p^{bat}_j + p^{def}_j + p^{shp}_j](l) + r_{ij}L_{ij}(l) \\ &\quad + \sum_{m:(j,m)\in\mathscr{L}} P_{jm}(l) + \sum_{d=0}^{d_{max}} z_d p^{new,d}_j(l) \end{aligned} \tag{25}$$

$$\begin{aligned} e^{bat}(N+k) &= \hat{e}^{bat}(N+k) \\ &\quad + \frac{1}{\eta}K^{shp}\left(e^{shp}_{des} - e^{shp}(N+k)\right) \\ &\quad + \sum_{r=N+k}^{k^{out}_{max}} \Delta T[p^{def} + \sum_{m=0}^{d_{max}} z_m p^{new,m}](r) \end{aligned} \tag{26}$$

The solution (x^*, u^*, z^*) of the Mixed Integer Program (MIP) (27) gives the optimal transition time $d^* = \sum_{m=0}^{d_{max}} m z^*_m$.

$$\min_{x,u,z} \quad V_3(u,z) = \sum_{m=0}^{d_{max}} m z_m \tag{27a}$$

$$\text{s.t} \quad x(l+1) = Ax(l) + Bu(l), \quad x_0 = x(0) \tag{27b}$$

$$(x(l), u(l), P_{ij}(l), Q_{ij}(l), V_i(l), L_{ij}(l)) \in \overline{\mathscr{Z}_l}$$

$$x(N+k) \in \overline{\mathbb{X}}_{N+k} \tag{27c}$$

$$z_m \in \{0,1\}\ \forall m \in \{0,1,...,d_{max}\}, \quad \sum_{m=0}^{d_{max}} z_m = 1 \tag{27d}$$

$$(25), (26) \tag{27e}$$

$$\begin{aligned} p_{j_{min}}{}^{bat} &\leq \hat{p}_j{}^{bat}(s) - [p^{def}_j + \sum_{m=0}^{d_{max}} z_m p^{new,m}_j](s) \\ &\quad - \frac{e^{shp}_{des,j} - e^{shp}_j(N+k)}{(k^{out}_j - (N+k))\eta} \end{aligned} \tag{27f}$$

$$\begin{aligned} e^{bat}_{max,j} &\geq \sum_{r=s}^{k^{out}_{max}} \Delta T[p_j{}^{def} + \sum_{m=0}^{d_{max}} z_m p^{new,m}_j](r) \\ &\quad + \frac{(e^{shp}_{des,j} - e^{shp}_j(N+k))(k^{out}_j - s)}{\eta(k^{out}_j - (N+k))} + \hat{e}^{bat}_j(s) \\ s &\in [N+k, k^{out}_j], \quad l = k, \ldots, k+N-1 \end{aligned} \tag{27g}$$

Objective (27a) minimizes the transition delay and ensures that the problem remains feasible when the load plugs in.

Remark 5. *Constraints (27f), (27g) correspond to the conditions in Lemma 1 Eq. (19), (20) respectively.*

We execute the request by (i) updating the system with the new load that plugs in at time d^*, and (ii) going back to *stage-2*. If $d^* > 0$, then the control devices and shapeable loads update their signal during the transition phase $[N+k, N+k+d^*]$. The full controller is shown in Fig. 2.

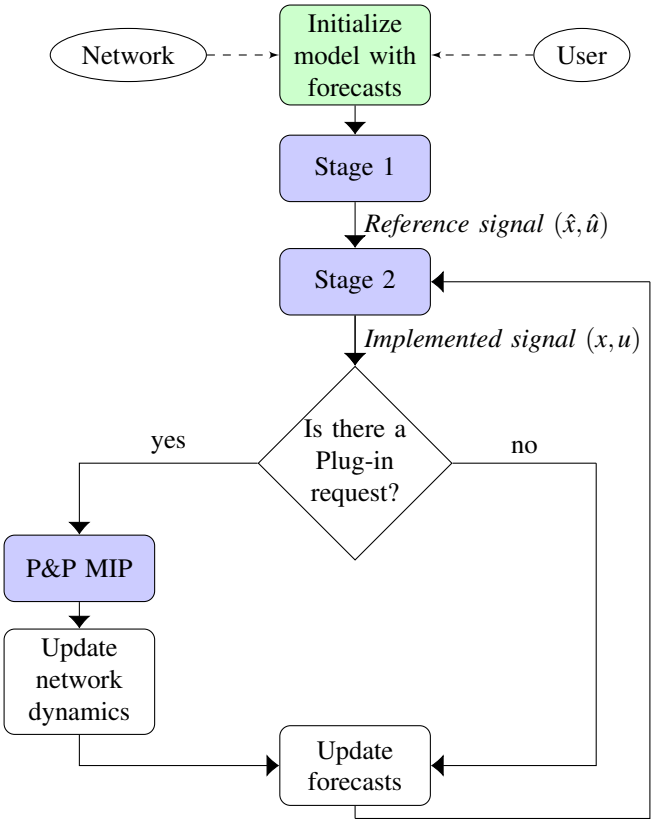

Fig. 2. Full controller flow: the solution at *stage-1* is used to define the terminal set at *stage-2*. When a new deferrable load requests to plug-in, the MIP determines the optimal plug-in time, the system is updated with the new load and the controller executes *stage-2* on the new system.

Theorem 1. *The model predictive controller (16) with network reconfigurations and transition times given by the MIP (27) is recursively feasible. For all initially feasible state x_0 and for all optimal sequences of control inputs, the MPC problem (16) with P&P network modifications (Fig. 2) remains feasible for all time.*

Proof. Assume the problem is feasible at time k and a request occurs at time k. The P&P MIP (27) ensures that all constraints are satisfied during the transition time and that the conditions in Lemma 1 are satisfied for the modified network. Hence the overall procedure maintains feasibility during transition, and recursive feasibility is ensured after the modification. □

V. Numerical Results

This section shows simulation results on a 55 bus Southern California Edison distribution network (see Fig. 3). This network was previously studied in [38]. Seven additional storage devices are modeled at nodes 2, 8, 10, 14, 21, 30, 41. We assume that the price of electricity is given and reflects the requirements of the system operator. In this case study, we choose the time step $\Delta t = 0.5$h, the *stage-2* MPC time horizon $\frac{N}{\Delta T}$ =5h and the *stage-1* time horizon $\frac{N_r}{\Delta T}$ =48h. The controller response is illustrated for a period of 30h in order to show daytime and night-time load schedules. These parameters are chosen for illustration purposes, and may be set differently to meet practical grid requirements. It is important to note that the choice of ΔT contains a tradeoff between reactivity and planning horizon. In particular, the controller response may be up to 30 minutes (ΔT) later than the request time of a load, and in practice, aggregators may require a smaller interval ΔT to reduce the response time and satisfy grid and users' requirements, however generally at the cost of not being able to plan optimally over a long time period of a day or more.

TABLE III
Description of Defferable Loads in the System

Request Time (h)	Requests	Bus number	Plug-in Time
4	1	8	4
6	1	33	6
10	5	4, 5, 5, 16, 17	10, 10, 10, 10, 10
11	1	28	11.5
12	2	19, 38	14.5, 12
17	3	8, 20, 22	17, 17, 17
18	1	12	18
18.5	2	5, 22	18.5, 18.5
19.5	1	12	19.5

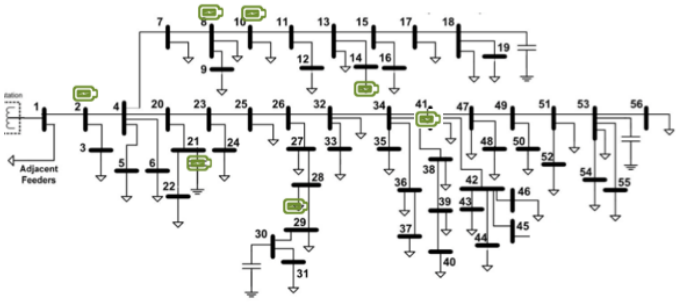

Fig. 3. 55 bus feeder. Additional battery banks are indicated in green (capacitors are not represented here).

A. Load scheduling

As mentioned in Section IV-A, shapeable loads plug-in as soon as they requests it, can be zero-power during a certain

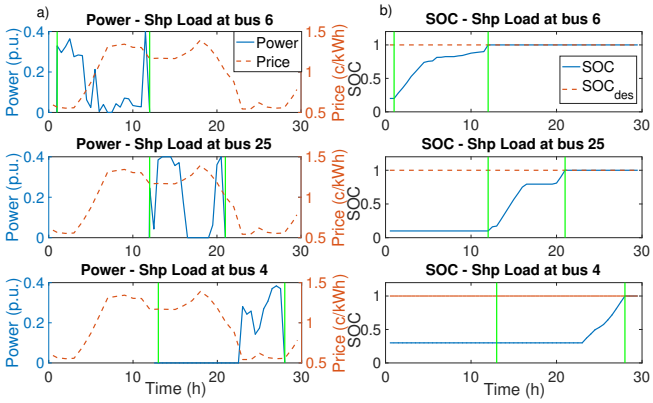

Fig. 4. Power and SOC of three different Shapeable Loads in the network. Green vertical lines show when the load requests to plug in and plug out.

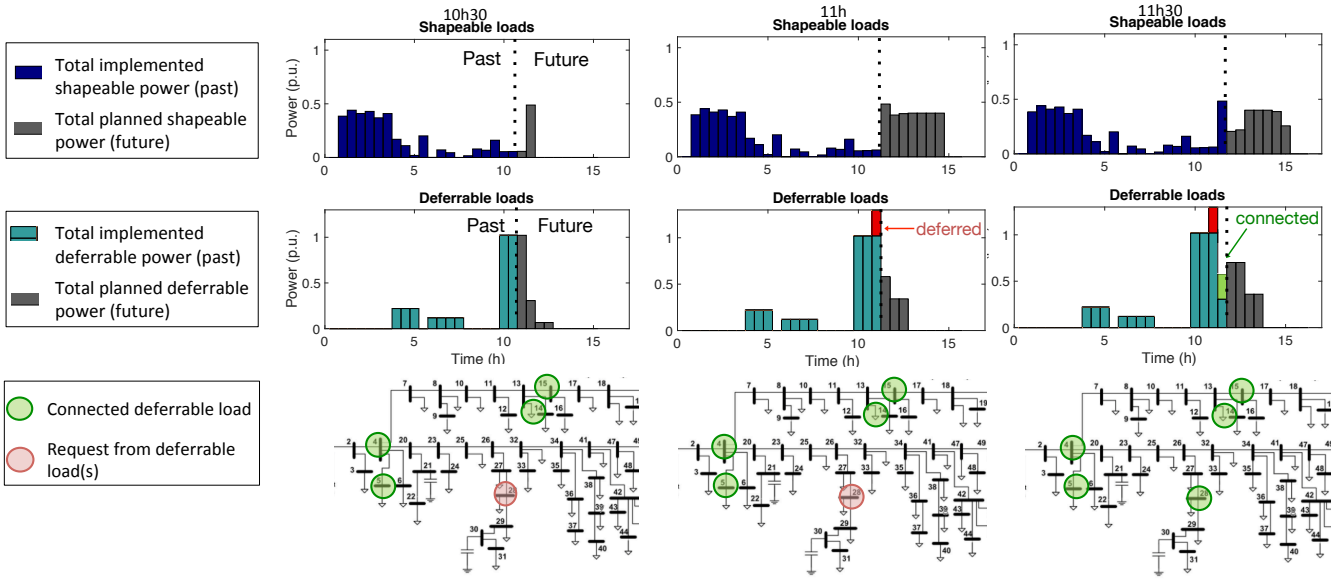

Fig. 5. Evolution of loads: one deferrable load requests to plug-in at 11h and is delayed to connect at 11h30. During the transition phase (11h-11h30), shapeable loads adapt their signal to enable safe connection of the deferrable load.

time and fully charge before their desired plug-out time k^{out}. Figure 4 shows the power and SOC at three shapeable loads. The vertical green lines show the connected period: the first green line is the request time, the second green line is k^{out}. Figure 4a shows that loads draw power only when they are plugged-in and Fig. 4b shows that they reach their desired SOC before k^{out}. In these three examples, the loads tend to charge when the price of electricity is cheaper. In particular, the load at bus 4 avoids the evening peak time (5pm to 9pm), and charges during the night time (10pm to 6am). Shapeable loads have the flexibility to adapt their power signal to the conditions and constraints of the network. In particular, they can adapt their response when a deferrable load requests to plug-in, allowing the new load to connect without violating the network constraints. Table III details all the plug-in requests and shows that only two deferrable loads need to be deferred in this case: one load at time 11h and bus 28 and one load at time 12h and bus 19. Figure 5 shows the overall state of the system when the deferrable load is delayed at 11h. It shows the total implemented and planned loads (shapeable in the top plot and deferrable in the middle plot) before and after the delayed request. During the transition phase (11h-11h30), shapeable loads adapt their signal, i.e. reduce their demand, to enable safe connection of the deferrable load at 11h30.

B. Peak reduction impact

In this section the peak reduction impact of the controller is illustrated. Figure 6 shows the aggregate load in the network in three cases: a) in the uncontrolled case, b) when the controller is applied to the network with deferrable and shapeable loads and c) when the controller is applied to the network without deferrable loads. In the uncontrolled case, every load plugs in as soon as it requests it. The total peak in the uncontrolled case (Fig. 6a) is 3.5 p.u. whereas it is 2 p.u in the controlled case (Fig 6b), providing 40% reduction. In the uncontrolled case, a lot of additional loads plug-in during the peak time (3pm to 9pm) and immediately charge. On the contrary, in the controlled case, shapeable loads are delayed to the night time, which results in a smoother load curve. The difference between Fig. 6b and Fig. 6c illustrates how shapeable loads' schedules change when deferrable loads are connected to the network. Fig 6b shows that shapeable loads adapt their load profile to enable connection of deferrable loads: in Fig 6b shapeable power tends to be delayed to the night time, in order to allow connection of deferrable loads in the evening (6pm to 9pm).

C. Network constraints

Network constraints include voltage and battery banks constraints. Figure 7 illustrate the voltage at each bus and time step and shows that voltage remains between the bounds 0.95 and 1. Figure 8 shows the power and SOC at the seven battery banks and Fig. 9 shows the aggregated real power over time. Figure 8a shows that batteries tend to highly discharge, i.e. have high negative power, around 10h, 15h and 20h. Figure 9 shows that these are times when the network is highly loaded, i.e. a lot of shapeable loads and deferrable loads are connected and fixed loads are high. Storage devices are used to supply additional power in case of load peaks. Note that we impose the minimum SOC, $e^{bat}_{low} = 0.12$ however the SOC never goes below 0.3. This limit is due to the terminal constraints (15b): the initial SOC has to be recoverable at the final time $N_h = 48h$. Fig 10 and Fig 11 show the output of *stage-1*, for capacitors and batteries respectively. We use a different color scale to highlight that the variation is very different from the *stage-2* response. Indeed, the objective in *stage-1* penalizes large control inputs whereas the objective in *stage-2* penalizes large peak consumptions, as a result the input in *stage-1* is lower than in *stage-2*. Fig 11 a) and b) show that the SOC at battery banks remains between 0.42 and 0.57. Batteries supply energy around 15h (peak consumption) and consume energy during

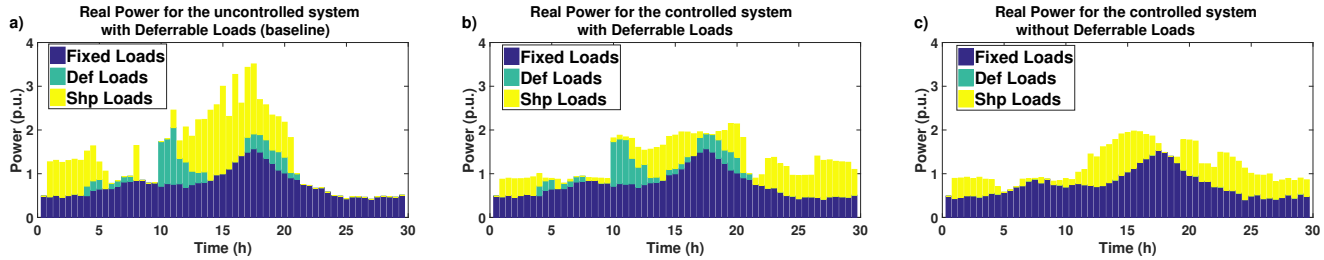

Fig. 6. Cumulative real power in the network for a) the uncontrolled system with deferrable loads, b) the controlled system with deferrable loads, c) the controlled system without deferrable loads

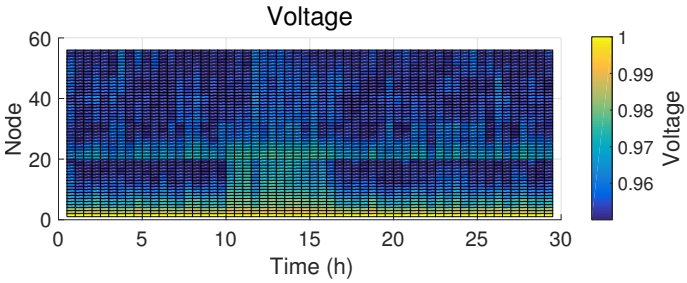

Fig. 7. Voltage at each mode of the network

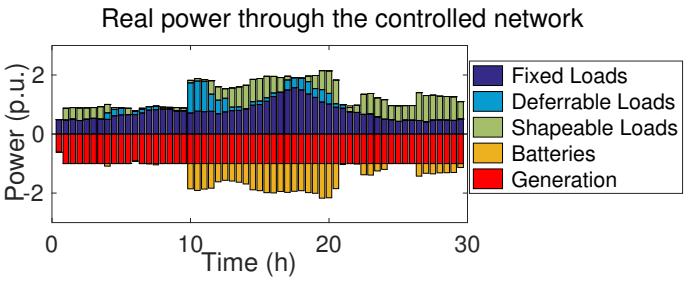

Fig. 9. Real power across the different devices of the networks

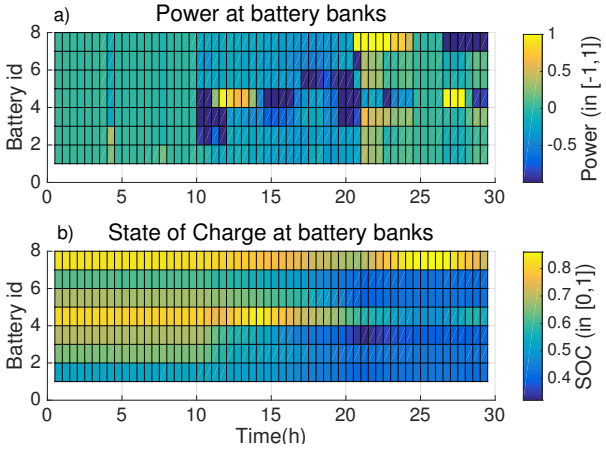

Fig. 8. a) Real power and b) SOC at battery banks. Values are normalized

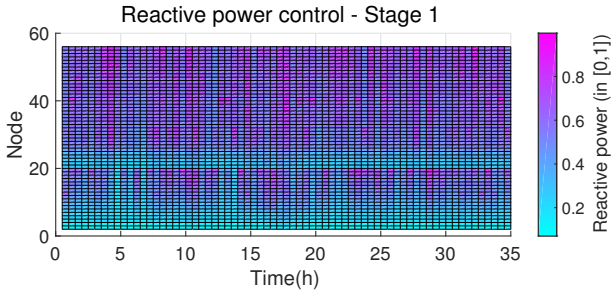

Fig. 10. Capacitor reactive power computed at Stage 1

the night to be able to recover the initial SOC. This *stage-1* response is used as a reference signal in *stage-2*.

VI. Conclusion

In this paper, a predictive controller capable of handling P&P requests of flexible and deferrable loads, is proposed. First, an MPC approach for minimizing the global cost of the system is used to aggregate flexible loads and provide load shaping objectives under distribution grid constraints. Second, a MIP is defined to safely connect loads and minimize waiting times. The article proved that the algorithm achieves recursive feasibility, by appropriately defining the connection conditions and the terminal constraint set. The performance of the proposed method was demonstrated for the control of a radial distribution system with 55 buses.

References

[1] W. Wang, Y. Xu, and M. Khanna, "A survey on the communication architectures in smart grid," *Computer Networks*, vol. 55, no. 15, pp. 3604–3629, 2011.

[2] P. Palensky and D. Dietrich, "Demand side management: Demand response, intelligent energy systems, and smart loads," *IEEE Transactions on Industrial Informatics*, vol. 7, no. 3, pp. 381–388, 2011.

[3] C. W. Gellings, *The smart grid: enabling energy efficiency and demand response*. The Fairmont Press, Inc., 2009.

[4] C. Le Floch, F. Belletti, S. Saxena, A. Bayen, and S. Moura, "Distributed optimal charging of electric vehicles for demand response and load shaping," in *54th Annual Conference on Decision and Control*, 2015.

[5] H. Lund and W. Kempton, "Integration of renewable energy into the transport and electricity sectors through V2G," *Energy policy*, vol. 36, no. 9, pp. 3578–3587, 2008.

[6] D. B. Richardson, "Electric vehicles and the electric grid: A review of modeling approaches, impacts, and renewable energy integration," *Renewable and Sustainable Energy Reviews*, vol. 19, pp. 247–254, 2013.

[7] W. Kempton and J. Tomić, "Vehicle-to-grid power fundamentals: Calculating capacity and net revenue," *Journal of power sources*, vol. 144, no. 1, pp. 268–279, 2005.

[8] A. Langton and N. Crisostomo, "Vehicle-grid integration: A vision for zero-emission transportation interconnected throughout california's electricity system," California Public Utilities Commission, Tech. Rep.

[9] C. Le Floch, F. Belletti, S. Saxena, A. M. Bayen, and S. Moura, "Distributed optimal charging of electric vehicles for demand response and load shaping," in *2015 54th IEEE Conference on Decision and Control (CDC)*. IEEE, 2015, pp. 6570–6576.

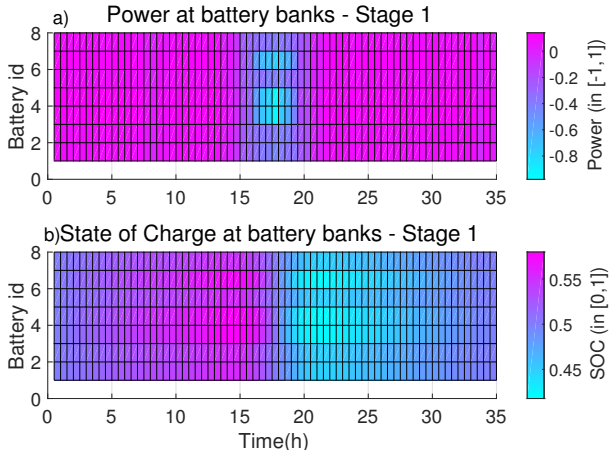

Fig. 11. a) Real power and b) SOC at battery banks computed at Stage 1 (values are normalized)

[10] L. Gan, U. Topcu, and S. H. Low, "Optimal decentralized protocol for electric vehicle charging," *IEEE Transactions on Power Systems*, vol. 28, no. 2, pp. 940–951, 2013.

[11] Z. Ma, D. Callaway, and I. Hiskens, "Decentralized charging control for large populations of plug-in electric vehicles," in *49th IEEE conference on decision and control (CDC)*. IEEE, 2010, pp. 206–212.

[12] W.-J. Ma, V. Gupta, and U. Topcu, "On distributed charging control of electric vehicles with power network capacity constraints," in *2014 American Control Conference*. IEEE, 2014, pp. 4306–4311.

[13] Y. Mou, H. Xing, Z. Lin, and M. Fu, "Decentralized optimal demand-side management for PHEV charging in a smart grid," *IEEE Transactions on Smart Grid,*, vol. 6, no. 2, pp. 726–736, 2015.

[14] F. Delfino, R. Minciardi, F. Pampararo, and M. Robba, "A multilevel approach for the optimal control of distributed energy resources and storage," *IEEE Transactions on Smart Grid*, vol. 5, no. 4, pp. 2155–2162, 2014.

[15] S. Deilami, A. S. Masoum, P. S. Moses, and M. A. Masoum, "Real-time coordination of plug-in electric vehicle charging in smart grids to minimize power losses and improve voltage profile," *IEEE Transactions on Smart Grid*, vol. 2, no. 3, pp. 456–467, 2011.

[16] J. Soares, M. A. F. Ghazvini, Z. Vale, and P. de Moura Oliveira, "A multi-objective model for the day-ahead energy resource scheduling of a smart grid with high penetration of sensitive loads," *Applied Energy*, vol. 162, pp. 1074–1088, 2016.

[17] M. F. Shaaban, M. Ismail, E. F. El-Saadany, and W. Zhuang, "Real-time pev charging/discharging coordination in smart distribution systems," *IEEE Transactions on Smart Grid*, vol. 5, no. 4, pp. 1797–1807, 2014.

[18] J. A. P. Lopes, F. J. Soares, and P. M. R. Almeida, "Integration of electric vehicles in the electric power system," *Proceedings of the IEEE*, vol. 99, no. 1, pp. 168–183, 2011.

[19] S. Riverso, F. Sarzo, and G. Ferrari-Trecate, "Plug-and-play voltage and frequency control of islanded microgrids with meshed topology," *IEEE Transactions on Smart Grid*, vol. 6, no. 3, pp. 1176–1184, 2015.

[20] M. N. Zeilinger, Y. Pu, S. Riverso, G. Ferrari-Trecate, and C. N. Jones, "Plug and play distributed model predictive control based on distributed invariance and optimization," in *52nd IEEE Annual Conference on Decision and Control, 2013*, pp. 5770–5776.

[21] J. Stoustrup, "Plug & play control: Control technology towards new challenges," *European Journal of Control*, vol. 15, no. 3, 2009.

[22] S. Bansal, M. N. Zeilinger, and C. J. Tomlin, "Plug-and-play model predictive control for electric vehicle charging and voltage control in smart grids," in *Conference on Decision and Control*, 2014.

[23] M. Farivar and S. H. Low, "Branch flow model: Relaxations and convexification—part i," *IEEE Transactions on Power Systems*, vol. 28, no. 3, pp. 2554–2564, 2013.

[24] M. Dong, P. C. Meira, W. Xu, and C. Chung, "Non-intrusive signature extraction for major residential loads," *IEEE Transactions on Smart Grid*, vol. 4, no. 3, pp. 1421–1430, 2013.

[25] J. Z. Kolter and M. J. Johnson, "Redd: A public data set for energy disaggregation research," in *Workshop on Data Mining Applications in Sustainability (SIGKDD), San Diego, CA*, vol. 25. Citeseer, 2011, pp. 59–62.

[26] Z. Li, Q. Guo, H. Sun, and J. Wang, "Storage-like devices in load leveling: Complementarity constraints and a new and exact relaxation method," *Applied Energy*, vol. 151, pp. 13–22, 2015.

[27] C. Le Floch, F. Belletti, and S. Moura, "Optimal charging of electric vehicles for load shaping: a dual splitting framework with explicit convergence bounds," *IEEE Transactions on Transportation Electrification*, 2016.

[28] Y. He, B. Venkatesh, and L. Guan, "Optimal scheduling for charging and discharging of electric vehicles," *IEEE Transactions on Smart Grid*, vol. 3, no. 3, pp. 1095–1105, 2012.

[29] J. Hu, S. You, M. Lind, and J. Ostergaard, "Coordinated charging of electric vehicles for congestion prevention in the distribution grid," *IEEE Transactions on Smart Grid*, vol. 5, no. 2, pp. 703–711, 2014.

[30] M. E. Baran and F. F. Wu, "Optimal sizing of capacitors placed on a radial distribution system," *IEEE Trans. on Power Delivery*, vol. 4, no. 1, pp. 735–743, 1989.

[31] M. Farivar, L. Chen, and S. Low, "Equilibrium and dynamics of local voltage control in distribution systems," in *52nd IEEE Annual Conference on Decision and Control (CDC), 2013*, pp. 4329–4334.

[32] M. E. Baran and F. F. Wu, "Optimal capacitor placement on radial distribution systems," *IEEE Trans. on Power Delivery*, vol. 4, no. 1, pp. 725–734, 1989.

[33] P. P. Barker and R. W. De Mello, "Determining the impact of distributed generation on power systems. i. radial distribution systems," in *Power Engineering Society Summer Meeting, 2000. IEEE*, vol. 3. IEEE, 2000, pp. 1645–1656.

[34] Y. Liu, J. Bebic, B. Kroposki, J. De Bedout, and W. Ren, "Distribution system voltage performance analysis for high-penetration pv," in *Energy 2030 Conference, 2008. ENERGY 2008. IEEE*. IEEE, 2008, pp. 1–8.

[35] L. N. Trefethen and D. Bau III, *Numerical linear algebra*. Siam, 1997, vol. 50.

[36] C. Le Floch, S. Bansal, C. J. Tomlin, S. Moura, and M. Zeilinger, "Plug-and-Play Model Predictive Control for Load Shaping and Voltage Control in Smart Grids," *ArXiv e-prints*, no. 1606.06682, Jun. 2016.

[37] S. Riverso, M. Farina, and G. Ferrari-Trecate, "Plug-and-play decentralized model predictive control for linear systems," *IEEE Trans. on Automatic Control*, vol. 58, no. 10, pp. 2608–2614, 2013.

[38] M. Farivar, C. R. Clarke, S. H. Low, and K. M. Chandy, "Inverter VAR control for distribution systems with renewables," in *IEEE International Conference on Smart Grid Communications, 2011*, pp. 457–462.